# Geochemical processes in a highly acidic pit lake of the Iberian Pyrite Belt (SW Spain).

C.R. Cánovas[a b], S. Peiffer[c], F. Macías[d], M. Olías[b], J.M. Nieto[d]

a) Department of Biology, Faculty of Marine and Environmental Sciences, University of Cádiz, Pol. Rio San Pedro s/n, 11510 Puerto Real, Cadiz, Spain.

b) Department of Geodynamics and Palaeontology, Faculty of Experimental Sciences, University of Huelva, Campus el Carmen s/n, 21071 Huelva, Spain.

c) Department of Hydrology, Bayreuth Center of Ecology and Environmental Sciences–BayCEER, University of Bayreuth, Universitätsstrasse 30, 95440 Bayreuth, Germany,

d) Department of Geology, Faculty of Experimental Sciences, University of Huelva, Campus el Carmen s/n, 21071 Huelva, Spain.

Corresponding author:

E-mail address: carlos.ruiz@dgeo.uhu.es (C.R. Cánovas).

Tel.:+34 959219870; fax: +34 959 219834

## *Abstract*

Compared with pit lakes originated by coal mining, little is known about in-lake neutralization processes in pit lakes from sulfide ore mining in hard rock substrates, which are typically very deep and acidic and receive low carbon (C) inputs and groundwater flows. Physicochemical processes in water and sediments from a pit lake (San Telmo, 130 m deep) in the Iberian Pyrite Belt were investigated. San Telmo is a meromictic and highly acidic (pH 2.8) pit lake due to pH buffering by precipitation of Fe(III) minerals (schwertmannite and jarosite). The sediments have a low abundance of C (below 0.60%) and iron minerals (below 0.12%) compared to most coal-mining pit lakes. In San Telmo sediments, iron reduction and sulfide oxidation may be thermodynamically favoured due to low pH values in pore waters (below 3.8) and the

presence of reactive iron. Although schwertmannite is the main ferric mineral precipitating in the water column, mineralogical analyses reveal a low abundance of schwertmannite in the sediment. This may be due to the preferential use of this mineral in reduction reactions mediated by bacteria, together with a low replenishment rate of the schwertmannite pool in the sediment. The transformation of reactive iron (schwertmannite and jarosite) into goethite may limit sulfate reduction, promoting acidic conditions in the sediment. As long as the acid mine drainage continues to discharge into the lake, the pH buffering exerted by ferric minerals in the sediments will limit the neutralization of the pH by sulfate reduction.

**Keywords:** San Telmo pit lake, schwertmannite transformation, pH buffering, iron and sulfate reduction, alkalinity generation.

## 1. Introduction and scope

The Iberian Pyrite Belt (IPB) is one of the most important polymetallic sulfide-mining regions in the world. Mining activity in the IPB dates back to prehistoric times, specifically to the third millennium B.C., and developed to such a magnitude that it provoked an unprecedented impact on the environment (Nocete et al., 2005). The long history of metalliferous mining in the region has left a legacy of derelict mines and an enormous amount of mining wastes, including sulfide-bearing waste rock piles, tailings, and so on. The oxidation of sulfides and consequent production of acid mine drainage (AMD), has provoked intense pollution of the main fluvial systems draining the IPB: the Tinto and Odiel rivers (e.g. Olías et al., 2006; Sánchez-España et al., 2005; Cánovas et al., 2007; Sarmiento et al., 2009a). The enormous pollution caused by mining wastes deposited over the centuries remains active and will continue to generate acid mine drainage for a long time to come (Younger et al., 2002).

From the second half of the nineteen century, underground workings and opencast mining in the IPB were used simultaneously in order to exploit the mineral deposits more efficiently. In the IPB, the existence of more than 30 mine pit lakes has been recorded, many of them flooded during the second half of the twentieth century, concomitant with the decline of mining activities in the region (Sánchez-España et al., 2008). During exploitation, the water table is suppressed to avoid the flooding of active mines. However, when the mining activity ceases, the water table recovers its original position, flooding the open pits and giving rise to mine pit lakes. The rise of the water table promotes the oxidative dissolution of sulfides contained in the pit banks, interconnected underground galleries, and shafts, which may cause water acidification and the subsequent dissolution of gangue minerals from the host rocks. In many cases, water stored in pit lakes is of poor quality and may contain concentrations of metals that greatly exceed water quality standards. In this respect, the Water Framework Directive (WFD) of the European Union (EC 2000) considers mining lakes as artificial surface water bodies which have to be monitored and managed to reach an acceptable water quality status. Achieving this goal requires the implementation of remediation strategies that need to be supported by a deep knowledge of the physicochemical processes and interactions between the water column and lake sediments. Most research has focused on lakes from coal mining (e.g. Küsel, 2003; Blodau and Knorr, 2006; Schultze et al., 2010) which receive high organic C inputs and are an integral part of the regional groundwater flow system, typically unconsolidated sandy aquifers, with large flow rates. In-lake neutralization processes in these systems are generally well known. Schwertmannite formation by Fe(II) oxidation and accumulation in the sediment promotes the occurrence of an acidic iron cycle that suppresses sulfate reduction (e.g. Peine et al., 2000; Blodau, 2004; Blodau and Gatzek, 2006). Proton-consuming sulfate reduction in sediments has been reported to occur at pH values between 4 and 5 (e.g. Küsel, 2003). Therefore, neutralization processes rely on the shift from an iron to a sulfate reductive environment. In coal pit lakes, this is largely driven by groundwater

dynamics (e.g. Blodau and Knorr, 2006; Neumann et al., 2013) depending on the advective input of alkalinity and acidity or electron acceptors and donors.

However, little is known about in-lake neutralization processes in acid pit lakes formed from sulfide ore mining, which are typically very deep, meromictic and receive low C inputs and groundwater flow because they are located in hard rock environments. A recent study (Wendt-Potthoff et al., 2012) was performed on alkalinity-producing processes in the shallower meromictic lake of Cueva de la Mora (40 m deep) located near San Telmo. In this sense, San Telmo Pit Lake can be considered as a reference example for in-depth study of factors controlling internal neutralization processes in pit lakes resulting from sulfide ore mining. This study is therefore aimed at providing information on physicochemical processes in the water and sediments from San Telmo Pit Lake, which is necessary as a starting point for evaluating the best remediation options in the long term.

## 2. Material and Methods

### 2.1. Site description

Despite the fact that mining activity in the San Telmo mining district dates back thousands of years, the more intense period of mining began in 1859 and continued until 1960, during which around 17 Mt of mineral were obtained (Pinedo Vara, 1963). Since then, approximately 15 Mt more was produced until the mine closure in 1989. Intense opencast mining activities that developed in San Telmo gave rise to a pit of around 130 m depth, which was progressively flooded by water table recovery after the cessation of mining. The water reached the overflow level in 1995, and the pit lake obtained its present configuration (Fig. 1A). A bathymetric study performed in 2005 shows a maximum depth of 130 m in the pelagic zone (Fig. 1C), accounting for total dimensions of 580 × 375 × 130 m, which represented the largest volume of acidic waters stored in

107 the IPB until the recent flooding of the Corta Atalaya open pit at Riotinto, the greatest
108 opencast sulphide mine in Europe (1200 × 900 × 350 m). The rapid flooding of San
109 Telmo Pit Lake is due to its location within the drainage area of the Fresnera Stream
110 (Fig. 1B). San Telmo Pit Lake is also fed by mining lixiviates coming from the intersecting
111 galleries: runoff generated from rainfall episodes, and lixiviates originating from the
112 washout of mining wastes placed in the vicinity of the pit lake.

113 2.2. Sampling and field measurements

114 Sediment and water sampling was performed in June 2006 in San Telmo Pit Lake. A
115 vertical profile was also carried out to measure temperature ($T^a$), pH, redox potential,
116 dissolved oxygen (DO), electrical conductivity (EC), and turbidity by means of a SEBA
117 Hydrometrie KLL-Q multi-probe. Electrodes were previously calibrated with calibration
118 standard solutions. Redox potential values were corrected to obtain the potential referred
119 to the hydrogen electrode (Nordstrom and Wilde, 1998).

120 Three water samples (0, 40, and 123 m) were collected along the water column
121 according to changes in EC. Water samples were filtered (0.45 μm), acidified with $HNO_3$
122 to a pH below 2, cooled at 4 ºC, and stored in the dark until analysis. A 60 cm sediment
123 core was taken by a UWITEC™ gravity corer from the pelagic zone at around 123 m,
124 sealed, and cooled to avoid oxidation processes until analysis.

125 2.3. Water and pore water analysis

126 Lake water was analysed in the Central Research Services of the University of Huelva
127 by using a Jobin Yvon (JY ULTIMA 2) optical spectrometer (ICP-OES). The method used
128 is especially designed to estimate major, minor, and trace elements in water affected by
129 acid mine drainage (Ruiz et al., 2003). The reliability of the measurements was verified
130 with certified reference material (SRM® NIST 1640). A triplicate analysis was performed
131 in order to evaluate the precision, which was better than 5% in all cases. In each analysis
132 sequence, internal standards were used to check the accuracy. Blanks were also

analysed with all elements below the detection limit of the equipment. Pore water was collected from different layers of sediment by centrifugation (at 10000 rpm for 15 minutes at around 4 ºC), and pH, Eh, and temperature were immediately measured. Ferrous and total iron concentrations were analysed following the phenanthroline method (Rodier et al., 1996). Arsenic, Pb, and Zn in pore waters were also analysed by atomic absorption spectroscopy (AAS) at the University of Bayreuth. All analyses were run in triplicate.

### 2.4. Sediment Analysis

The core was cut into into diametral sections of 3 cm thick by a UWITEC slicer, weighed, and subsequently frozen to avoid oxidation processes. Before analysis, samples were dried by a freeze-dryer and subsequently weighed and placed in storage. Sample oxidation was prevented using an inert gas glove box during sample handling. The water content was obtained from the difference between wet and dry sediment weights. Reactive Fe was determined after digesting the sample with HCl 1 N and shaking for 24 h according to Wallmann et al. (1993). Reactive Fe denotes the fraction that easily undergoes chemical or microbial dissolution and can therefore be regarded as potentially available for microbial reduction (Canfield, 1989). Total Fe was also measured in sediments using HCl 6 N as the digestion solution. Digestates were analysed by ICP-OES in triplicate for statistical purposes. Other elements such as Al, As, Cd, Co, Cu, Cr, Mn, Ni, Pb, and Zn were also analysed.

Sulfur speciation analyses were carried out at the Department of Hydrology of Bayreuth University. Total Reduced Inorganic Sulfur (TRIS, composed of $FeS_2$, FeS, and Sº) was analysed photometrically by the methylene blue method (Budd and Bewick, 1952) after hot acid digestion and subsequent reduction with $Cr(II)Cl_2$ to $H_2S$. Elemental sulfur (Sº) was analysed by high-pressure chromatography and UV-detector (Ferdelman et al., 1991) after extraction with methanol. Total sulfur and C were analysed using a C-S LECO Analyser by combustion at 1300 ºC.

159 Different techniques were used to identify mineral phases in sediments. No treatment
160 was applied to samples before measurements. Transmittance of infrared radiation
161 (between wave numbers 450 and 4500) was measured by Fourier Transform Infrared
162 Spectroscopy (FTIR) at the Limnological Station of Bayreuth University. Samples were
163 also measured by X-ray diffraction (XRD) using a Bruker D8 Advance diffractometer with
164 Cu Kα radiation at the Central Research Services of the University of Huelva. As a
165 consequence of the low crystallinity of mineral phases in sediments, the scan period was
166 increased from 3 to 65º 2Θ with a continuous scan at a rate of 0.025º 2Θ/18 s. Samples
167 were also observed by Scanning Electronic Microscope with an Energy Dispersive
168 System (SEM-EDS) using a JEOL JMS-5410 instrument at the University of Huelva.

169 2.5. Data treatment

170 Diffusive fluxes of Fe(II) and Zn from the sediment to the water column were calculated
171 from Fick's first law of diffusion:

172 $$D_J = \frac{-\theta}{\gamma^2} D \frac{\Delta C}{\Delta x}, \qquad \text{Eq. 1}$$

173 where Θ is the porosity of the shallowest slice of the core (0–3 cm) calculated from the
174 weight difference after centrifugation and $\gamma$ is the tortuosity calculated from the porosity
175 according to Boudreau (1996). D is the diffusion coefficient for each element obtained
176 by the method of Li and Gregory (1974), and ΔC/Δx is the concentration gradient between
177 the shallowest sediment and the overlying waters.

178 The saturation indices of water samples and the speciation of the main elements in the
179 lake waters were calculated using the geochemical code PHREEQC (Parkhurst and
180 Appelo, 1999). The thermodynamic database of PHREEQC was augmented with data
181 for the solubility of schwertmannite (Bigham et al., 1996: log $K_{sp}$ = 18.0 ± 2.5; Yu et al.,
182 1999: log $K_{sp}$ = 10.05 ± 2.5) and ferrihydrite (MINTEQA2; Allison et al., 1990). Redox
183 potential (pE) was used as the master variable to characterize all equilibria related to Fe

184 species. In acidic solutions that contain sufficient concentrations of ferrous and ferric iron
185 (> $10^{-5}$ M), measured pE values reflect the redox equilibrium between $Fe^{2+}$ and $Fe^{3+}$
186 (Grundl and Macalady, 1989).

187

188 **3. Results**

189 3.1. Water column and pore waters

190 The evolution of physicochemical parameters along the water column is shown in Figure
191 2. The San Telmo Pit Lake is meromictic (Diez-Ercilla et al., 2009), with a 29-m-deep
192 oxygenated and lower-density layer (mixolimnion) and a 100-m-deep anoxic and higher-
193 density layer (monimolimnion; Fig. 2). Mixolimnetic waters are slightly stratified: a
194 warmer and lighter epilimnion (0–3 m), a transitional metalimnion (3–10 m), and a lower
195 and cooler hypolimnion (10–29 m) are observed (Fig. 2). This stratification of the
196 mixolimnion is progressively formed at the beginning of the spring and disappears during
197 the winter, when mixing takes places (Diez-Ercilla et al., 2009). The mixolimnetic waters
198 show more oxidative conditions and lower EC values (807–883 mV; 5.3 mS/cm) than
199 monimolimnetic waters (650 mV; 6.6 mS/cm). San Telmo waters have high acidity, with
200 almost constant pH values of around 2.8 throughout the water column. The turbidity
201 ranged from 3 to 5 NTU (Fig. 2), with higher values in the upper 5 m (11 NTU), at the
202 halocline (9.3 NTU), and close to the bottom of the lake (20 NTU). However, the highest
203 values were observed at the water–sediment interface (close to 1000 NTU) due probably
204 to the abundance of resuspended colloids. High concentrations of sulfate (3963–4227
205 mg/L) and metals (e.g. 139–163 mg/L of Fe, 81–90 mg/L of Zn, 23–25 mg/L of Cu, and
206 223–237 µg/L of Cd) were recorded in the water column, reaching the highest values in
207 the monimolimnion (Table 1).

208 An increase in pH values was observed at the water–sediment interface compared with
209 those recorded in the lake water (from 2.8 to 3.3). This increase continued in the

sediment pore waters, reaching a maximum value of 3.8 at the bottom (Fig. 3). The opposite trend was observed for Eh: a decrease from 633 to 455 mV was recorded from the water column to the sediment bottom. The concentration of dissolved Fe increased sharply at the water–sediment interface in relation to the water column (from 163 to 2024 mg/L) but decreased progressively in pore waters with sediment depth (down to 963 mg/L of Fe; Fig. 3). Ferrous iron followed a similar trend to total Fe (from 1671 to 801 mg/L) in pore waters. The concentration of Zn at the sediment–water interface was twice that recorded in the lake water (from 90 to 187 mg/L). However, Zn concentration fluctuated with sediment depth (Fig. 3). Arsenic was depleted from pore waters (below the detection limit of the equipment) in relation to the water column (around 64 μg/L; Table 1). This depletion was also observed for Pb at the sediment–water interface and in the upper 6 cm of sediments. However, concentrations of Pb above 100 μg/L were recorded in the 6–12 cm core section, decreasing thereafter towards the bottom sediment.

### 3.2. Sediments

Visually, the sediment cores could be divided into two different zones. The upper 10 cm contained brownish orange sediments with a dry weight of around 40% (Table 2). Downwards, the sediment had a yellowish brown colour with decreasing water content due to compaction by burial by newly settled particles. A low content of total C (below 0.60%), decreasing with sediment depth (from 0.56 to 0.12%; Table 2), was observed in the sediment. All C can be considered as organic due to the acidic conditions found in the sediment (pH below 4). The highest concentration of reactive iron ($Fe_r$) was found in the upper 3 cm of the sediments (around 25 g/kg) and decreased with depth (Table 2). Total Fe ($Fe_t$) concentrations ranged from 120 g/kg at the top to 25 g/kg between 15 and 18 cm. According to these data, the $Fe_r/Fe_{tot}$ ratio decreased from 21 to 10% with sediment depth.

236 The total S ($S_{tot}$) content ranged from 27 to 78 g/kg of sediment (Table 2), reaching the
237 highest values between 15 and 18 cm. The content of TRIS ($FeS_2$, FeS, and Sº) in the
238 sediments ranged from 0.90 to 9.0 g/kg, with the highest values found between 15 and
239 18 cm. The concentrations of elemental sulfur (Sº) were generally low (from 0.007 to
240 0.027 mg/kg; Table 2) except in the upper centimetres of the sediments (0.167 mg/kg).
241 Acid volatile sulfur (FeS) was not analysed. The large difference between total (27–78
242 g/kg) and reduced S (0.9–9.0 g/kg) may be due to the high abundance of sulfate and
243 oxyhydroxysulfate in the sediments.

244 The XRD profiles of the sediments (Fig. 4) reveal the predominance of detrital minerals
245 (e.g. quartz, muscovite, illite, clinochlore) common in pelitic and volcanic host rocks
246 outcropping in the area. Despite the oversaturation predicted by PHREEQC in
247 mixolimnetic waters (IS 4.7; Table 3) the presence of schwertmannite in the sediments
248 could not be confirmed by XRD, probably due to its low crystallinity in relation to detrital
249 minerals. However, a detailed microscopic examination of sediments by SEM-EDS
250 revealed the presence of schwertmannite, with its typical “pin cushion” morphology, in
251 the surface sediments (Fig. 5A). On the other hand, several peaks corresponding to
252 jarosite were identified in the XRD profiles; their intensity decreased with sediment depth
253 (Fig. 4). The opposite tendency was observed for pyrite; a higher abundance of this
254 mineral was recorded in the deeper sediment layers (Fig. 4). This mineral distribution
255 was confirmed by SEM-EDS; a high abundance of detrital pyrite and iron oxides (Fig. 5C
256 and D) was observed in the deeper sediment. In contrast, a higher presence of
257 schwertmannite was observed in the top sediment layer (Fig. 5A). The presence of
258 sulfates (i.e. barite and anglesite) was also documented by SEM-EDS (Fig. 5A).

259 The FTIR spectra showed only slight changes with depth (Fig. 6). Based on studies in
260 other systems (e.g. Peine et al., 2000), changes due to the transformation of abundant
261 ferric iron mineral phases would be expected. However, Fe minerals are not predominant
262 components in San Telmo sediments (0.02 to 0.12 w%; Table 2), so their IR signals

seem to be diluted by other IR-sensitive compounds (e.g. clay minerals such as illite and clinochlore detected by XRD). In particular, the IR window between 850 and 1200 $cm^{-1}$, which covers many bands characteristic for AMD iron minerals (schwertmannite, goethite, and jarosite), seems to be hidden by other compounds. Nevertheless some conclusions can be drawn from the spectra with regard to the Fe geochemistry. There is some evidence for the occurrence of goethite: diagnostic bands are at 892 and 795 $cm^{-1}$. While the 892 $cm^{-1}$ band may be hidden under other vibration signals, the 795 $cm^{-1}$ band is clearly visible together with the 630 $cm^{-1}$ band (Fe-O symmetric stretch). The latter is indicative of a relatively high crystallinity (Cornell and Schwertmann, 2003), which may be due to transformation from metastable minerals (e.g. schwertmannite, Bigham et al., 1996; or jarosite, Acero et al., 2006). Even though SEM images suggest the occurrence of schwertmannite, there is only one band visible that is characteristic for this mineral (v3-vibration of sulfate at ~1190 $cm^{-1}$). This vibration is typically split into bands of higher vibration energy (~ 1120 and ~ 1050 $cm^{-1}$), which may be hidden behind the large signals of other compounds. However, the concentration of schwertmannite seems to be relatively low. The presence of jarosite, previously identified by XRD, is also supported by FTIR; the IR signals of jarosite (1005 and 1086 $cm^{-1}$) seem to be visible even within the large window covered by other compounds.

## 4. Discussion

### 4.1. Geochemical processes in the water column

San Telmo, like other lakes with a high relative depth, has developed meromixis (Sánchez-España et al., 2008). However this may not be the only cause; biological and physico-chemical factors can enhance meromixis. Primary production is limited in acidic mining lakes by the availability of inorganic C and P (Nixdorf et al., 2003). The most probable cause of meromixis in San Telmo is the input of waters with higher content of

289 dissolved solids from underground galleries. As can be seen in Table 1, higher
290 concentrations of Ca, Li, Mg, Mn, Na, $SO_4$, Sr, and Zn were recorded at depth. The
291 difference in temperature between the bottom of the mixolimnion and the monimolimnion
292 (around 1.1 ºC; Fig. 2) also suggests that this assumption is reasonable.

293 The oxidative dissolution of sulfides contained in the pit banks, interconnected
294 underground galleries, and mine wastes placed in the surroundings together with the
295 absence of acid-consuming rocks results in the input of a vast load of acidity, sulfate,
296 Fe(II), and accessory metals into the water column. The ferrous iron is subsequently
297 oxidized to ferric iron in the mixolimnion, which then precipitates, releasing acidity.
298 According to geochemical calculations with PHREEQC, around 99% of Fe is predicted
299 to occur as Fe(III) in the mixolimnetic waters and less than 7% in the monimolimnion.
300 The higher values of turbidity observed within the first 5 m of San Telmo waters may be
301 linked to Fe(III) precipitation (increasing colloidal Fe) and microbiological activity, as
302 highlighted by previous works dealing with San Telmo limnology (Sánchez-España et
303 al., 2007; Diez-Ercilla et al., 2009).

304 The almost constant values of pH in the water column suggest pH buffering consistent
305 to the precipitation of Fe(III) minerals. This control has been previously reported in
306 numerous acidic mining lakes with pH between 2.8 and 3.2 (e.g. Totsche et al., 2003;
307 Regenspurg et al., 2004; Pellicori et al., 2005). Geochemical calculations with
308 PHREEQC (Table 3) indicate oversaturation of mixolimnetic waters with respect to some
309 Fe(III)-containing minerals including schwertmannite, jarosite, and goethite. In
310 monimolimnetic waters, oversaturation with respect to jarositic minerals remains while
311 undersaturation is observed in the case of schwertmannite for both $K_{sp}$ used. However,
312 the appropriate $K_{sp}$ for schwertmannite solubility in natural systems is currently being
313 investigated due to its metastability and heterogeneous chemical composition. In this
314 sense, a recent paper by Caraballo et al. (2013) reports schwertmannite occurrence in
315 broad pH and pE ranges of 1.93–4.71 and 8.5–13.7, respectively, encouraging the use

316 of broader log $K_{sp}$ to model schwertmannite solubility for each specific environment.
317 Sánchez-España et al. (2011) report schwertmannite as the dominant phase
318 precipitating in the water column of San Telmo, although in contact with jarosite crystals.
319 The pH buffering throughout the entire water column by precipitation of Fe(III) minerals
320 has a sharp effect on metal mobility, allowing metals to remain dissolved. The low pH
321 values also inhibit the precipitation of Al minerals; only jurbanite is close to equilibrium
322 (Table 3), and this mineral is rarely found in AMD sites. The high concentration of sulfate
323 in San Telmo waters promotes the equilibrium with some sulfate minerals (i.e. barite,
324 gypsum; Table 3).

325 4.2. Geochemical processes in sediments

326 4.2.1. Mineral transformations and reduction reactions

327 The newly formed Fe(III) minerals (i.e. schwertmannite, jarosite) in the water column
328 settle and accumulate in the sediments, where they can undergo chemical
329 transformations. The XRD patterns and SEM images, together with the decrease in the
330 $Fe_r/Fe_t$ ratio with depth, indicate a downward decline of schwertmannite and jarosite with
331 sediment depth. This is consistent with the metastable nature of these minerals with
332 respect to goethite (Regenspurg et al., 2004). These overall reactions (Blodau, 2006)
333 generate acidity, helping to maintain low pH values in the sediment pore waters (Fig. 3),
334 and may release trace metals contained in the metastable minerals (Acero et al., 2006).

335 $$Fe_8O_8(OH)_6(SO_4) + 2H_20 \rightarrow 8FeOOH + 2H^+ + SO_4^{2-}$$ Eq. 2

336 The sharp increase in the Fe concentration of pore waters of San Telmo (Fig. 3) also
337 suggests the existence of Fe reduction in the sediment (Eq. 3). The reactivity of Fe(III)
338 minerals as electron acceptors for microbial processes is linked to their degree of
339 crystallinity (Peine et al., 2000). The low crystallinity of schwertmannite (not detected by
340 XRD or FTIR but observed by SEM) in San Telmo sediments points towards this mineral
341 as an easily available oxidant for microbial processes. The preferential utilization of

schwertmannite over jarosite by bacteria as an electron acceptor may explain its low abundance in San Telmo sediments, even though it is theoretically the main precipitating Fe compound. In this regard, Bridge and Johnson (2000) reported a faster reductive dissolution of schwertmannite than jarosite (and other iron oxides) by the catalysis of *Acidiphilium* SJH at pH 2.0–3.0. However, this hypothesis requires further study.

$$Fe_8O_8(OH)_6(SO_4) + 2CH_2O + 14H^+ \rightarrow 8Fe^{2+} + 2CO_2 + 12H_20 + SO_4^{2-} \quad \text{Eq. 3}$$

The reductive dissolution of schwertmannite would consume protons but release ferrous Fe, sulfate, and other metals (i.e. Zn and Pb) into the sediment pore waters (Fig. 3), and they can then diffuse into the overlying waters. Diffusive fluxes of 4.9 and 0.26 mol $m^2$ $s^{-1}$ of Fe(II) and Zn from San Telmo sediments to the water column were estimated, and these values are in agreement with fluxes reported for other acidic lakes (e.g. Peine et al., 2000; Blodau, 2004). In these acidic coal pit lakes (e.g. Peine et al., 2000; Blodau, 2004), the ferrous Fe diffused from the sediment was subsequently re-oxidized in the water column, giving rise to schwertmannite precipitation and thus enhancing an iron cycle in the sediment. In San Telmo Pit Lake, the monimolimnetic waters are permanently anoxic and Fe(II) re-oxidation may be inhibited, preventing the replenishment of the schwertmannite pool in the sediment.

On the other hand, the sulfate released is available for sulfate-reducing activity as observed in other AMD-affected reservoirs in the IPB (Sarmiento et al., 2009b; Torres et al., 2013) and worldwide (e.g. Herlihy et al., 1985; Blodau et al., 1998; Knöller et al., 2004; Meier et al., 2004). However, sulfate reduction does not seem to be a key process in San Telmo sediments: only 2 to 15% of total S is in the reduced form. Although AVS was not analysed, the high acidity found in the sediment probably maintains this S compound at very low levels. Elemental sulfur was found at low concentrations except in the superficial layer (Table 2), probably due to the oxidation of residual pyrite by Fe(III), releasing Fe(II) into the pore waters. Thus, the content of reduced sulfur of San Telmo

368 sediments may be mainly associated with its abundance in detrital pyrite, as evidenced
369 by the mineralogical results (i.e. XRD, SEM). The C content of San Telmo sediments is
370 rather low (total C below 0.6%; Table 2) with scarce availability of labile organic C, and
371 sulfate reduction (as well as Fe) must be C limited. Under this scenario, Fe and sulfate
372 reducers compete for the electron donor, and Fe reducing bacteria are
373 thermodynamically favoured in acidic sediments (Küsel et al., 1999) such as those found
374 in San Telmo. Other authors propose alternative mechanisms of sulfate reduction in
375 acidic environments. Koschorreck et al. (2003) reported active sulfate reduction at pH <
376 3 in the sediment of a volcanic lake (Lake Caviahue, Argentina). However, conditions
377 were significantly different from those found in San Telmo. The lake sediments received
378 high amounts of labile organic matter from algae killed by a volcanic eruption, and
379 potentially competing iron-reducing bacteria were probably inhibited by the low
380 availability of iron in the volcanic sediment. Koschorreck (2008) investigated the
381 existence of sulfate-reducing activity in acidic environments by calculating the energy
382 required to maintain a microniche of elevated pH around the bacteria. He concluded that
383 the high energy required makes these niches unlikely to persist in such acidic
384 environments.

385 4.2.2. Neutralization processes

386 The sediment pH needs to be maintained at near neutral values for an effective in-lake
387 neutralization through sulfate reduction and iron sulfide formation (Blodau and Peiffer,
388 2003; Küsel, 2003). The transformation of metastable Fe minerals (schwertmannite and
389 jarosite) into more stable minerals (goethite) may act as a pH buffer in San Telmo
390 sediments. Fe(III) reduction is strongly proton-consuming and energetically favourable
391 in acidic environments (Flynn et al., 2014), so the acidifying effect of schwertmannite
392 turns out to be critical for maintaining high rates of iron reduction and inhibiting sulfate
393 reduction in San Telmo. This buffering process has been previously documented in
394 acidic coal pit lakes (Peine et al., 2000; Blodau, 2004) and constitutes an acidic iron cycle

395 at the sediment–water interface. In these systems, the schwertmannite pool in the
396 sediment is replenished by Fe(II) reoxidation in the oxic water column, and therefore this
397 buffering is maintained. This is not the case for San Telmo, where Fe(II) generated by
398 reductive processes in the sediment diffuses into the anoxic monimolimnetic waters and
399 therefore is apparently not oxidized. As iron-reduction typically generates alkalinity, an
400 increase in the pH of the sediment pore waters should be expected. The question then
401 arises as to why this buffering exerted by Fe(III) mineral transformation is not overcome
402 by Fe reduction in San Telmo. A possible explanation could be the existence of an
403 additional source of acidity in the sediment by anaerobic oxidation of detrital pyrite, which
404 is abundant in San Telmo sediments. The occurrence of elemental S in the top sediment
405 layers suggests the existence of this reaction; however it seems unlikely that anaerobic
406 oxidation of pyrite could be a key reaction in sediment pH buffering because of the low
407 concentrations observed. Therefore the most probable explanation is the lack of
408 sufficient C in San Telmo sediments to generate alkalinity from reduction reactions that
409 would overcome the acidity generated by Fe(III) mineral transformation. This C limitation
410 is apparently overwhelmed in the nearby meromictic acidic pit lake of Cueva de la Mora
411 (Wendt-Potthoff et al., 2012) due to the high nutrient levels, which generate enough
412 organic C to promote sulfate reduction. However, the oligotrophic nature of San Telmo
413 waters limits the availability of organic C to enhance alkalinity production.

414 Another possible way of overcoming this buffering is through the input of alkalinity
415 sources. In some acidic coal pit lakes (e.g. Blodau and Knorr, 2006; Neumann et al.,
416 2013) an increase in pH with sediment depth was recorded and attributed to the inflow
417 of neutral Fe(II) and $SO_4$-rich groundwater, which promotes sulfate reduction. This
418 increase in pH also drives the conversion of schwertmannite to goethite (Eq. 2), which
419 leads to a depletion of reactive Fe, and therefore sulfate reduction can take place.
420 However, in San Telmo Pit Lake there is no such external driver (neutral groundwater
421 inflow) and therefore no sulfate reduction is observable. The current rates of Fe inputs

422 into the San Telmo Pit Lake, together with the low availability of organic C, must enhance
423 the preservation of the pH buffering in both the water column and the sediments.
424 Measures need to be taken to quantify and limit the Fe inputs into the pit lake and thus
425 inhibit the buffering effect of this metal on both the water column and the lake sediments.

426

427 **Conclusions**

428 The San Telmo Pit Lake is highly acidic (pH of 2.8) due to intensive sulfide oxidation
429 processes that occurred during its flooding. In the mixolimnion, ferrous iron is oxidized
430 to ferric iron, which then precipitates mainly as schwertmannite and jarosite, releasing
431 acidity, which results in pH buffering in the water column. The newly formed minerals
432 settle down in the sediment, where they may become converted upon burial to more
433 stable minerals such as goethite, releasing acidity. The higher concentration of Fe(II) in
434 the pore waters compared to the lake waters indicates the existence of Fe reduction.
435 Although schwertmannite is the main precipitating phase in the water column, its low
436 abundance in the sediment suggests the preferential use of this ferric mineral as an
437 electron acceptor by bacteria. This reaction consumes acidity and releases Fe(II) and
438 metals (e.g. Zn, Pb) into the pore waters, which diffuse into the overlying waters. The
439 alkalinity generated by Fe reduction in the sediments is insufficient to increase the pH
440 due to the buffering exerted by Fe mineral transformations, inhibiting sulfate reduction.
441 The content of total reduced inorganic sulfur (TRIS) oscillates between 2 and 15% of
442 total sulfur. The abundance of detrital pyrite in the sediment, as evidenced by XRD and
443 SEM analyses, points to this mineral as the main contributor of TRIS. Low concentrations
444 of $S^0$ were observed in the shallowest sediment layer and were probably formed by pyrite
445 oxidation by Fe(III). The availability of organic C limits the generation of alkalinity in the
446 sediment which could overcome the pH buffering exerted by Fe mineral transformation.
447 An investigation into the quantities of Fe and acidity entering the lake system is required

448 in order to quantify the mass balance of acidity and to predict the future evolution of San
449 Telmo waters and sediments. As long as the input of organic C, acidity, and iron into the
450 pit lake remains at similar rates, sulfate reduction will be inhibited.

451 **Acknowledgments**

452 This work has been financed through the projects CGL2013-48460-C2-1-R (Spanish
453 Ministry of Economy and Competitiveness) and P11-RNM-7199 (Andalusian Regional
454 Government). The Deutscher Akademischer Austausch Dienst (DAAD) provided
455 financial support for the stay of CRC at the University of Bayreuth. The authors gratefully
456 acknowledge the field assistance of Dr. Juan Antonio Morales and Dr. Joaquin Delgado,
457 and the technical support of Dr. Marcus Bauer, Dr. Klaus H. Knorr, Martin Back, Martina
458 Rohr, Isolde Baumann, Jutta Eckert and Karin Söllner (among others). The comments
459 and suggestions of the editor Carla M. Koretsky and two anonymous reviewers
460 significantly improved the original manuscript.

461

462 **References**

463 Acero, P., Ayora, C., Torrento, C., Nieto, J.M., 2006. The behavior of trace elements
464 during schwertmannite precipitation and subsequent transformation into goethite and
465 jarosite. Geochim. Cosmochim. Acta, 70, 4130-4139. doi:10.1016/j.gca.2006.06.1367

466 Allison, J.D., Brown, D.S., Novo-Gradac K.J., 1990. MINTEQA2/PRODEFA2. A
467 geochemical assessment model for environmental systems. V 3.0. Environmental
468 Research Laboratory, Office of Research and Development, U.S. Environmental
469 Protection Agency. Athens, Georgia. 106 pp.

470 Bigham, J.M., Schwertmann, U., Traina, S.J., Winland, R.L., Wolf, M., 1996.
471 Schwertmannite and the chemical modeling of iron in acid sulfate waters. Geochim.
472 Cosmochim. Acta, 60(12), 2111-2121.

473 Blodau, C., Hoffmann, S., Peine, A., Peiffer, S. 1998. Iron and sulfate reduction in the
474 sediments of acid mine lake 116 (Brandenburg, Germany): rates and geochemical
475 evaluation. Water Air Soil Pollut. 108, 249–270.

476 Blodau, C., Peiffer, S., 2003. Thermodynamics and organic matter: constraints on
477 neutralization processes in sediments of highly acidic waters. Appl. Geochem. 18 (1),
478 25–36.

479 Blodau, C., 2004. Evidence for a hydrologically controlled iron cycle in acidic and iron
480 rich sediments. Aquat. Sci. 66, 47–59.

481 Blodau, C., 2006. A review of acidity generation and consumption in acidic coal mine
482 lakes and their watersheds. Sci. Total Environ. 369, 307–332.
483 doi:10.1016/j.scitotenv.2006.05.004.

484 Blodau C., Gatzek C., 2006. Chemical controls on iron reduction rates in
485 schwertmannite-rich sediments. Chem. Geol. 235, 366-376.
486 doi:10.1016/j.chemgeo.2006.08.003

487 Blodau, C., Knorr, K.H., 2006. Experimental inflow of groundwater induces a
488 “biogeochemical regime shift” in iron-rich and acidic sediments, J. Geophys. Res., 111,
489 *G02026, doi:*10.1029/2006JG000165.

490 Boudreau B.P, 1996. The diffusive tortuosity of fine-grained unlithified sediments.
491 Geochim Cosmochim Acta 60, 3139–3142.

492 Bridge, T.A.M., Johnson, D.B., 2000. Reductive Dissolution of Ferric Iron Minerals by
493 Acidiphilium SJH. Geomicrobiol. J., 17(3), 193-206. doi: 10.1080/01490450050121161.

494 Budd, M.S., Bedwick, H.A., 1952. Photometric determination of sulphide and reducible
495 sulphur in alkalises. Anal. Chem., 24, 1536-1540.

496 Canfield, D.E., 1989. Reactive iron in marine sediments. Geochim. Cosmochim. Acta 53,
497 619–632.

498 Cánovas, C.R., Olias, M., Nieto, J.M., Sarmiento, A.M., Cerón, J.C., 2007.
499 Hydrogeochemical characteristics of the Odiel and Tinto rivers (SW Spain). Factors
500 controlling metal contents. *Sci. Total Environ.,* 373, 363-382.
501 doi:10.1016/j.scitotenv.2006.11.022.

502 Caraballo, M.A, Rimstidt, J.D, Macías, F., Nieto, J.M, Hochella, M.F.,
503 2013. Metastability, nanocrystallinity and pseudo-solid solution effects on the
504 understanding of schwertmannite solubility. Chem. Geol. 360-361, 22-31. doi:
505 10.1016/j.chemgeo.2013.09.023

506 Cornell, R.M., Schwertmann, U., 2003. The Iron Oxides: Structure, Properties,
507 Reactions, Occurrences and Uses.

508 Diez Ercilla, M., Lopez Pamo E., Sanchez España, J., 2009. Photoreduction of Fe(III) in
509 the Acidic Mine Pit Lake of San Telmo (Iberian Pyrite Belt): Field and Experimental Work.
510 Aquat. Geochem., 15, 391-419. doi: 10.1007/s10498-008-9044-1

511 EC Decision 2000/60/EC. Council Decision of 23 October 2000 establishing a
512 communitarian frame of action in the scope of water policy. Official Journal L 327,
513 22/12/2000, pp. 1-88.

514 Ferdelman, T.G., Church, T.M., Luther, G.W. 1991. Sulfur enrichment of humic
515 substances in a Delaware salt marsh sediment core. Geochim. Cosmochim. Acta 55,
516 979–988.

517 Flynn T.M, O'Loughlin E.J., Mishra B., DiChristina T.J., Kemner K.M. 2014. Sulfur-
518 mediated electron shuttling during bacterial iron reduction. Science 344, 1039-1042. doi
519 10.1126/science.1252066

520 Grundl, T.J, Macalady, D.L., 1989. Electrode measurement of redox potential in
521 anaerobic ferric/ferrous chloride systems. J Contam. Hydrol. 5, 97-117.

522 Herlihy, A.T., Mills, A.L., 1985. Sulfate reduction in freshwater sediments receiving acid
523 mine drainage. Appl. Environ. Microbiol. 49, 179–186.

524 Knöller, K., Fauville, A., Mayer, B., Strauch, G., Friese, K., Veizer, J., 2004. Sulfur cycling
525 in an acid mining lake and its vicinity in Lusatia, Germany. Chem. Geol. 204, 303–323.
526 doi:10.1016/j.chemgeo.2003.11.009

527 Koschorreck M., Wendt-Potthoff K., Geller W., 2003. Microbial sulfate reduction at low
528 pH in sediments of an acidic lake in Argentina. Environ. Sci. Technol. 37, 1159–1162.
529 doi: 10.1021/es0259584

530 Koschorreck, M., 2008. Microbial sulphate reduction at a low pH. *FEMS Microbiol.*
531 *Ecol.*, 64 (3), 329-342. doi:10.1111/j.1574-6941.2008.00482.x

532 Küsel, K., Dorsch, T., Acker, G., Stackebrandt, E., 1999. Microbial reduction of Fe(III) in
533 acidic sediments: Isolation of Acidiphilium cryptum JF-5 capable of coupling the
534 reduction of Fe(III) to the oxidation of glucose. Appl. Environ. Microbiol. 65, 3633–40.

535 Küsel, K., 2003. Microbial cycling of iron and sulfur in acidic coal mining lake sediments.
536 Water Air Soil Pollut., Focus 3 (1), 67–90. doi: 10.1023/A:1022103419928

537 Li, Y.H, Gregory, S., (1974). Diffusion of ions in sea water and in deep-sea sediments.
538 Geochim. Cosmochim. Acta 38, 703–714

539 Meier, J., Babenzien, H.D., Wendt-Potthoff, K., 2004. Microbial cycling of iron and sulfur
540 in sediments of acidic and pH-neutral mining lakes in Lusatia (Brandenburg, Germany).
541 Biogeochemistry 67, 135–156.

542 Neumann, C., Beer, J., Blodau, C., Peiffer, S., Fleckenstein, J.H., 2013. Spatial patterns
543 of groundwater-lake exchange – implications for acid neutralization processes in an acid
544 mine lake. Hydrol. Process. 27, 3240–3253. doi: 10.1002/hyp.9656.

545 Nixdorf, B., Lessmann, D., Steinberg, C.E.W., 2003. The importance of chemical
546 buffering for pelagic and benthic colonization in acidic waters. Water Air Soil Pollut., 3,
547 27–46. doi: 10.1023/A:1022111605815

548 Nocete, F., Alex, E., Nieto, J.M., Sáez, R., Bayona, M.R., 2005. An archaelogical
549 approach to regional environmental pollution in the south-western Iberian Peninsula
550 related to Third Millenium B.C mining and metallurgy. Journal of Archaeological Science,
551 32 (10), 1566-1576. doi:10.1016/j.jas.2005.04.012

552 Nordstrom, D.K., Wilde, F.D., 1998. Reduction–oxidation potential (electrode method),
553 in National Field Manual for the Collection of Water Quality Data, book 9, chapter 6.5, 20
554 pp., U.S. Geological Survey techniques of water-resources investigations, U.S.
555 Geological Survey, Reston, Va.

556 Olías, M., Cánovas, C., Nieto, J.M., Sarmiento, A.M., 2006. Evaluation of the dissolved
557 contaminant load transported by the Tinto and Odiel rivers (South West Spain). Appl.
558 Geochem., 21, 1733-1749. doi:10.1016/j.apgeochem.2006.05.009

559 Parkhurst, D.L., Appelo, C.A.J., 1999. User's Guide to PHREEQC (Version 2) A
560 Computer Program for Speciation, Batch-Reaction, One-Dimensional Transport, and
561 Inverse Geochemical Calculations, USGS Water-Resources Investigations, Denver,
562 Colorado.

563 Peine, A., Tritschler, A., Küsel, K., Peiffer, S., 2000. Electron flow in an iron-rich acidic
564 sediment—evidence for an acidity-driven iron cycle. Limnol. Oceanog. 45, 1077–1087.
565 doi: 10.4319/lo.2000.45.5.1077

566 Pellicori, D.A., Gammons, C.H., Poulson, S.R., 2005. Geochemistry and stable isotope
567 composition of the Berkeley pit lake and surrounding mine waters, Butte, Montana. Appl.
568 Geochem. 20, 2116–2137. doi:10.1016/j.apgeochem.2005.07.010

569 Pinedo Vara I., 1963. Piritas de Huelva. Su historia, minería y aprovechamiento. Summa.
570 Madrid, Spain. 1003 pp.

571 Regenspurg, S., Brand, A., Peiffer, S., 2004. Formation and stability of schwertmannite
572 in acidic pit lakes. Geochim. Cosmochim. Acta 68, 1185–1197.
573 doi:10.1016/j.gca.2003.07.015

574 Rodier, J., Broutin, J.P., Chambon, P., Champsaur, H., Rodi, L., 1996. L'analyse de
575 l'eau, Dunod, Paris.

576 Ruiz, M.J., Carrasco, R., Pérez-López, R., Sarmiento, AM., Nieto, J.M., 2003.
577 Optimización del análisis de elementos mayores y traza mediante UN-ICP-OES en
578 muestras de drenaje ácido de mina. Proceedings of IV Iberian Geochemical Meeting,
579 14-18 Julio. Coimbra, Portugal. Universidad de Coimbra. 402–404.

580 Sánchez España, J., Lopez Pamo, E., Santofimia, E., Aduvire, O., Reyes, J., Barettino,
581 D., 2005. Acid mine drainage in the Iberian Pyrite Belt (Odiel river watershed, Huelva,
582 SW Spain): Geochemistry, mineralogy and environmental implications. Appl. Geochem.
583 20, 1320-1356. doi:10.1016/j.apgeochem.2005.01.011

584 Sánchez-España J., Santofimia E., González-Toril, E., San Martín-Uriz, P., López Pamo
585 E., Amils, R., 2007. Physicochemical and microbiological stratification of a meromictic,
586 acidic mine pit lake (San Telmo, Iberian Pyrite Belt). In: Cidu, R., Frau, F. (Eds.),
587 Proceedings Symposium International Mine Water Association (IMWA'2007), Italy, 28–
588 31 May 2007, Cagliari, Sardinia, Italy, pp. 447–451.

589 Sánchez-España, J., López-Pamo, E., Santofimia, E., Diez, M., 2008. The acidic mine
590 pit lakes of the Iberian Pyrite Belt: An approach to their physical limnology and

591 hydrogeochemistry. Appl. Geochem., 23, 1260-1287. doi:
592 10.1016/j.apgeochem.2007.12.036

593 Sánchez-España, J., Yusta, I., Diez-Ercilla, M., 2011. Schwertmannite and
594 hydrobasaluminite: A re-evaluation of their solubility and control on the iron and
595 aluminium concentration in acidic pit lakes. Appl. Geochem. 26, 1752-1774.
596 doi:10.1016/j.apgeochem.2011.06.020

597 Sarmiento, A.M., Nieto, J.M., Olías, M., Cánovas, C.R., 2009a. Hydrochemical
598 characteristics and seasonal influence on the pollution by acid mine drainage in the Odiel
599 river Basin (SW Spain). Appl. Geochem. 24, 697-714.
600 doi:10.1016/j.apgeochem.2008.12.025

601 Sarmiento, A.M., Olías, M., Nieto, J.M., Cánovas, C.R., Delgado, J., 2009b. Natural
602 attenuation processes in two water reservoirs receiving acid mine drainage. Sci Total
603 Environ, 407: 2051–62. doi:10.1016/j.scitotenv.2008.11.011

604 Schultze, M., Pokrandt, K.H., Hille, W., 2010. Pit lakes of the Central German lignite
605 mining district: Creation, morphometry and water quality aspects. Limnologica 40. 148-
606 155. doi:10.1016/j.limno.2009.11.006.

607 Torres, E., Ayora, C., Canovas, C.R., García-Robledo, E., Galván, L., Sarmiento, A.M.
608 2013. Metal cycling during sediment early diagenesis in a water reservoir affected by
609 acid mine drainage. Sci. Total Environ., 461-462, 416-429. doi:
610 10.1016/j.scitotenv.2013.05.014

611 Totsche, O., Pöthig, R., Uhlmann, W., Büttcher, H., Steinberg, E.W., 2003. Buffering
612 mechanisms in acidic mining lakes—a model-based analyses. Aquat. Geochem. 9, 343–
613 359.

614 Wallmann, K., Hennies, K., König, K.I., Petersen, W., Knauth, H.D., 1993. New
615 procedure for determining reactive Fe(III) and Fe(II) minerals in sediments. Limnol.
616 Oceanogr. 38, 1803–1812.

617 Wendt-Potthoff, K., Koschorreck, M., Diez, M., Sánchez-España, J., 2012. High
618 microbial activity in a nutrient-rich, acidic mine pit lake. Limnologica 42–3, 175–188.
619 doi:10.1016/j.limno.2011.10.004.

620 Younger, P.L., Banwart, S.A., Hedin, R.S., 2002. Mine water. Hidrology, Pollution,
621 Remediation. Environmental Pollution. Kluwer Academic Publishers. Dordrecht. Vol. 5,
622 442 pp.

623 Yu, J.Y., Heo, B., Choi, I.K., Cho, J.P., Chang, H.W., 1999. Apparent solubilities of
624 schwertmannite and ferrihydrite in natural stream waters polluted by mine drainage.
625 Geochim. Cosmochim. Acta, 63(19/20), 3407-3416.

626 **TABLES**

| | | Depth (m) | | |
|---|---|---|---|---|
| | | 0 | 40 | 123 |
| Al | *Main Elements (mg/L)* | 129 | 132 | 128 |
| Ca | | 213 | 237 | 259 |
| Cu | | 23 | 24 | 25 |
| Fe | | 163 | 139 | 163 |
| K | | 2.9 | 2.2 | 2.7 |
| Mg | | 422 | 480 | 554 |
| Mn | | 40 | 41 | 48 |
| Na | | 17 | 19 | 19 |
| Sulfate | | 3963 | 4011 | 4227 |
| Si | | 30 | 28 | 29 |
| Zn | | 81 | 86 | 90 |
| As | *Trace elements (µg/L)* | 64 | n.a. | 35 |
| Ba | | 3.4 | 2.7 | 6.2 |
| Be | | 20 | 21 | 23 |
| Cd | | 223 | 229 | 237 |
| Co | | 970 | 754 | 1262 |
| Cr | | 13 | 13 | 16 |
| Li | | 440 | 463 | 807 |
| Ni | | 445 | 437 | 515 |
| Pb | | 93 | n.a. | 61 |
| Sr | | 261 | 309 | 359 |

627

628 **Table 1.** Chemical composition of San Telmo pit lake waters at different depths (n.a: not
629 analysed).

| **Sediment depth** (cm) | **$H_20$** % | **C tot** % | **$Fe_r$** g/kg | **$Fe_t$** g/kg | **TRIS** g/kg | **$S^o$** mg/kg | **S tot** g/kg |
|---|---|---|---|---|---|---|---|
| 0 - 3 | 0.63 | 0.56 | 25 | 120 | 1.9 | 0.167 | 44 |
| 3 - 6 | 0.59 | 0.43 | 18 | 99 | 2.9 | 0.007 | 27 |
| 6 - 9 | 0.60 | 0.45 | 15 | 100 | 0.9 | 0.018 | 42 |
| 9 - 12 | 0.49 | 0.30 | 9.0 | 71 | 3.7 | 0.006 | 38 |
| 12 - 15 | 0.42 | 0.14 | 4.8 | 48 | 7.1 | 0.027 | 45 |
| 15 - 18 | 0.34 | 0.12 | 3.9 | 25 | 9.0 | 0.016 | 78 |

630

631 **Table 2.** Content of water, C, reactive and total Fe and main S species in
632 San Telmo sediments.

| | | Depth (m) | | |
|---|---|---|---|---|
| | | 0 | 40 | 123 |
| ***Al minerals*** | ***Formula*** | | | |
| Alunite | $KAl_3(SO_4)_2(OH)_6$ | -2.1 | -3.8 | -3.7 |
| Gibbsite | $Al(OH)_3$ | -3.6 | -4.4 | -4.4 |
| $Al(OH)_3$(a) | $Al(OH)_3$(a) | -6.3 | -7.2 | -7.2 |
| Jurbanite | $Al(SO_4)(OH)\cdot 5H_2O$ | -0.1 | 0.0 | 0.0 |
| Basaluminite | $Al_4(SO_4)(OH)_{10}\cdot 5H_2O$ | -12.9 | -12.7 | -12.8 |
| ***Sulfate minerals*** | | | | |
| Anglesite | $PbSO_4$ | -1.5 | - | -1.6 |
| Epsomite | $MgSO_4$ | -2.3 | -2.1 | -2.0 |
| Celestite | $SrSO_4$ | -1.6 | -1.5 | -1.4 |
| Barite | $BaSO_4$ | 2.5 | -0.4 | 0.0 |
| Gypsum | $CaSO_4$ | -0.1 | -0.3 | -0.3 |
| ***Fe minerals*** | | | | |
| Hematite | $Fe_2O_3$ | 11.4 | 8.8 | 8.3 |
| $Fe(OH)_3$(a) | $Fe(OH)_3$(a) | -1.2 | -2.0 | -2.3 |
| Goethite | FeOOH | 4.7 | 3.5 | 3.2 |
| Jarosite-K | $KFe_3(SO_4)_2(OH)_6$ | 4.3 | 2.0 | 1.2 |
| Jarosite-H | $HFe_3(SO_4)_2(OH)_6$ | 1.1 | -3.0 | -3.8 |
| Jarosite-Na | $NaFe_3(SO_4)_2(OH)_6$ | 0.5 | -2.9 | -3.7 |
| Schwertmannite(a) | $Fe_8O_8(OH)_{4.32}(SO_4)_{1.84}$ | -2.8 | -8.8 | -11.2 |
| Schwertmannite(b) | $Fe_8O_8(OH)_{4.32}(SO_4)_{1.84}$ | 4.7 | -1.3 | -3.7 |

(a) Ks according to Bigham et al. 1996

(b) Ks according to Yu et al. 1999

**Table 3.** Saturation indices (SI) of some minerals obtained by the PHREEQC code.

643 **FIGURES**

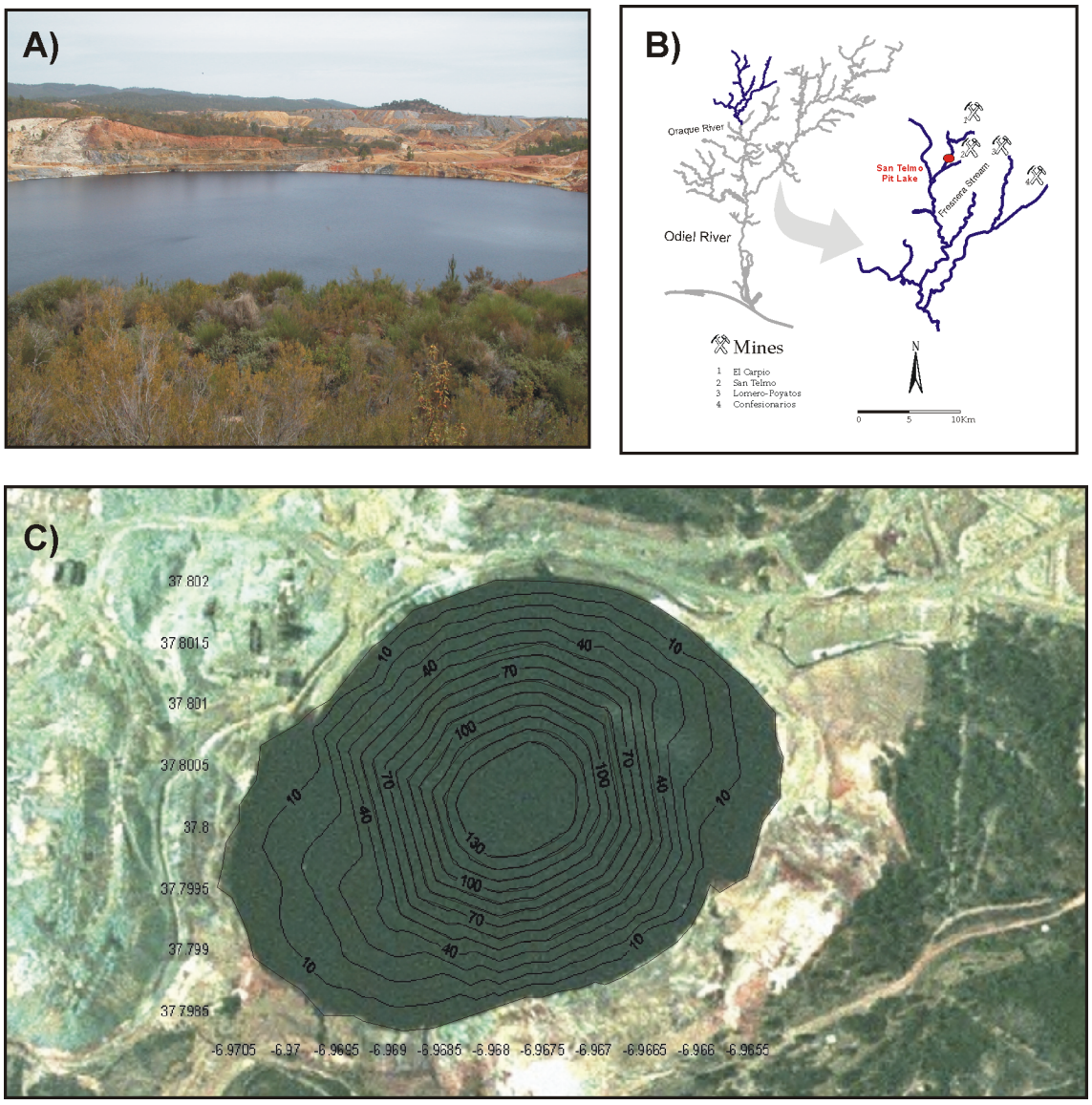


644

645 **Figure 1.** Panoramic view (A), location (modified from Sarmiento (2008) (B) and

646 bathymetry (C) of San Telmo Pit Lake (SW Spain).

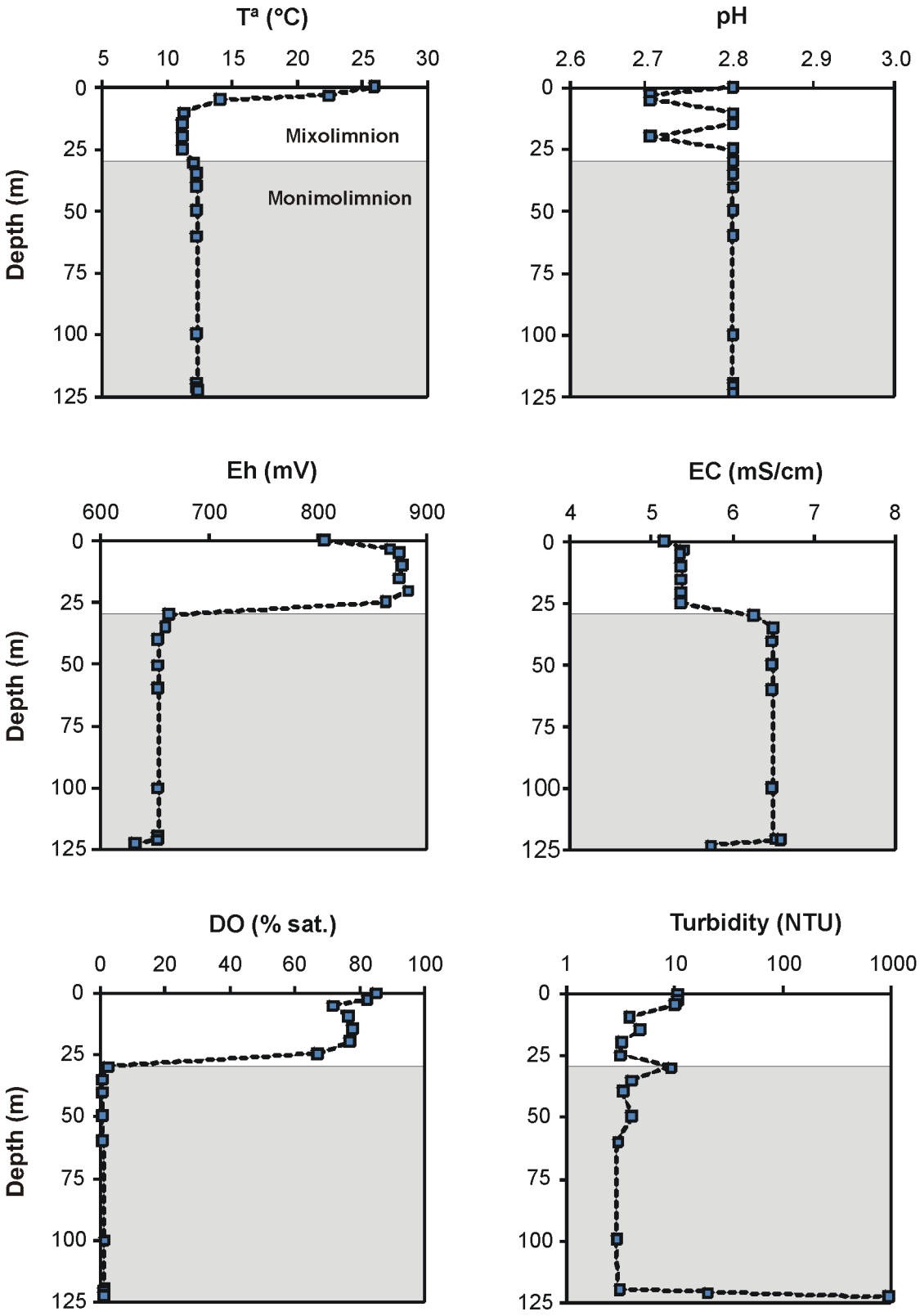


**Figure 2.** Vertical profile of main physico-chemical parameters in the water column of San Telmo Pit Lake.

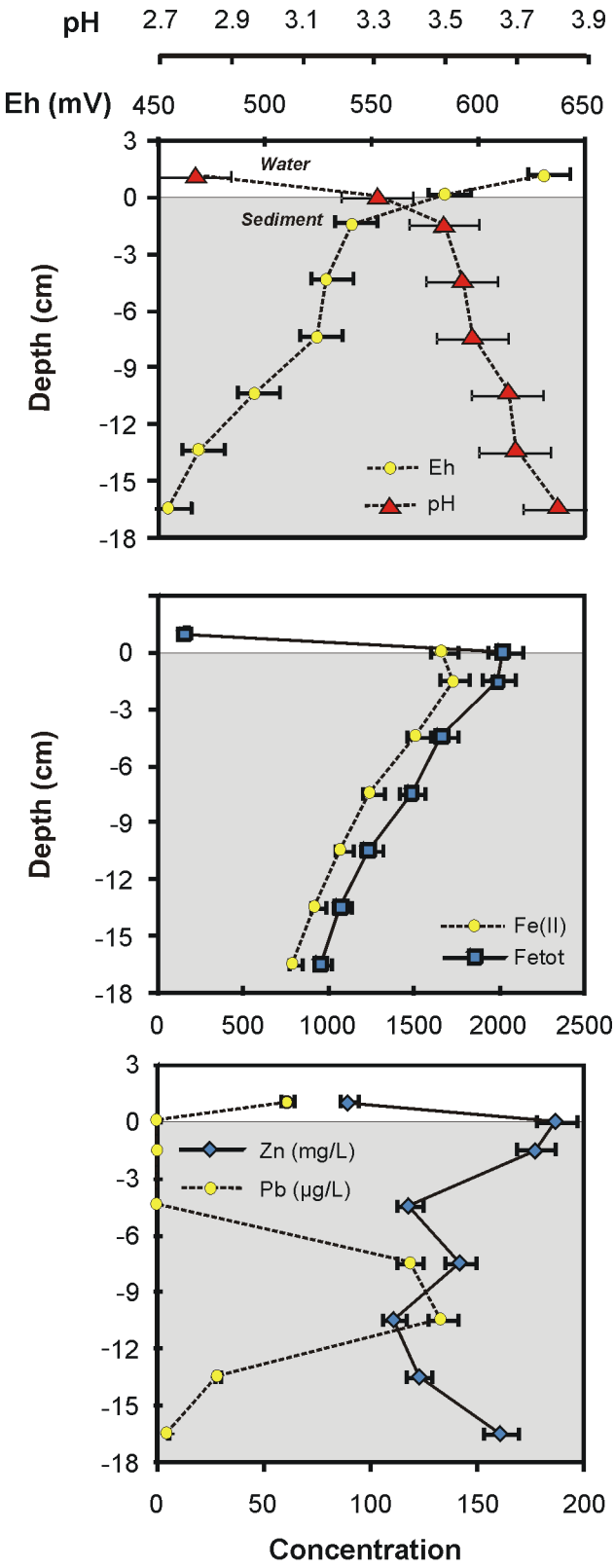


650

651 **Figure 3.** Profile of pH, Eh, Fe(II), total Fe, Pb and Zn in sediment pore waters of San

652 Telmo. Bars denote standard deviations.

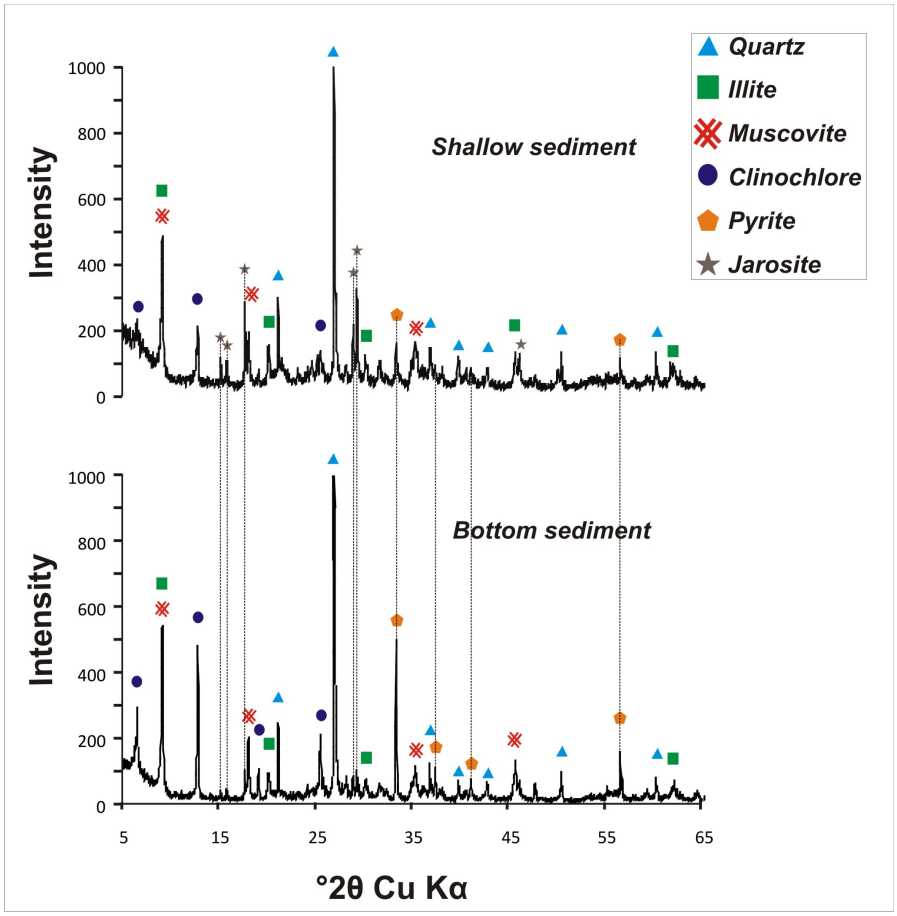


653

654 **Figure 4.** XRD profile of shallow (0-3 cm) and deep sediment (15-18 cm) highlighting the

655 minerals found.

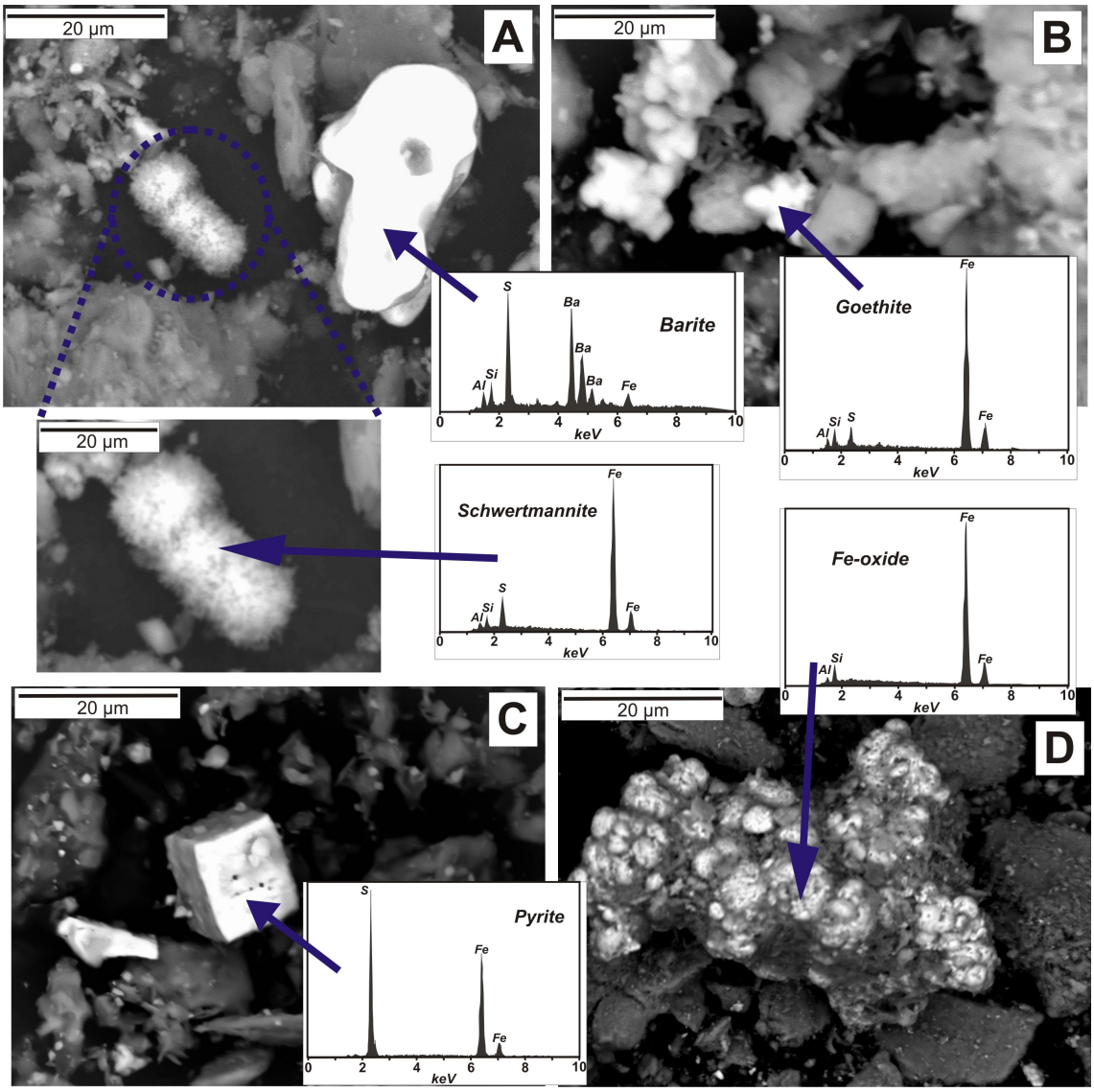


656

657 **Figure 5.** SEM images indicating the presence of barite, schwertmannite (A) and
658 goethite (B) in shallow sediments (0-3 cm), and pyrite (C) and Fe oxides (D) in deep
659 sediments (15-18 cm).

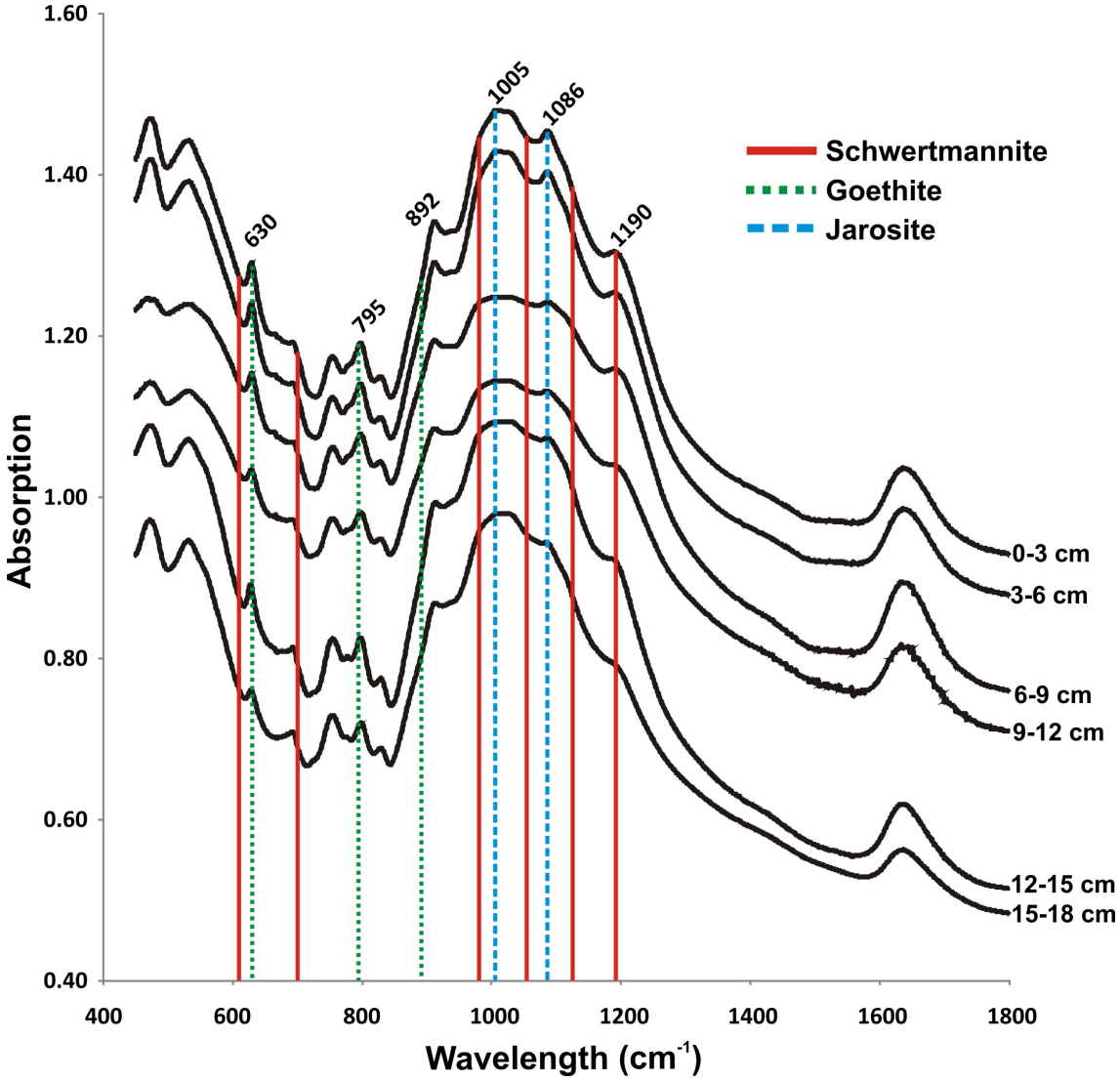


660

661 **Figure 6.** FTIR spectra of San Telmo pit lake sediments showing the characteristic bands

662 of schwertmannite, jarosite and goethite.

663

664